16) T. Shiokawa, Y. Hattori, K. Kawano, Y. Ohguchi, H. Kawakami, K.Toma, and Y. Maitani, Effect of the Polyethylene Glycol linker Chain Length of Folate-linked Microemulsions Loading Aclacinomycin A on Targeting Ability and Antitumor Effect in vitro and in vivo, Clinical Cancer Res, 11(5):2018-25 (2005).
17) Y. Maitani, K. Nakamura, K. Kawano. Application of sterylglucoside-containing particles for drug delivery. Curr. Pharm. Biotechnol, 6, 81-93 (2005).
18) M. Furuhata, H. Kawakami, K. Toma, Y. Hattori and Y. Maitani, Design, Synthesis and Gene Delivery Efficiencies of Novel oligo-Arginine Linked PEG-Lipid: Effect of Oligo-Arginine Length, Peptide Science 2004, 241-242, (2005).

Molecular Mobility of Nifedipine–PVP and Phenobarbital–PVP Solid Dispersions as Measured by ^{13}C-NMR Spin-Lattice Relaxation Time

YUKIO ASO, SUMIE YOSHIOKA

Division of Drugs, National Institute of Health Sciences, 1-18-1, Kamiyoga, Setagaya, Tokyo 158-8501, Japan

Received 1 January 2005; revised 15 April 2005; accepted 25 August 2005

Published online 21 December 2005 in Wiley InterScience (www.interscience.wiley.com). DOI 10.1002/jps.20545

ABSTRACT: Amorphous nifedipine–PVP and phenobarbital–PVP solid dispersions with various drug contents were prepared by melting and subsequent rapid cooling of mixtures of PVP and nifedipine, or phenobarbital. Chemical shifts and spin-lattice relaxation times (T_1) of PVP, nifedipine, and phenobarbital carbons were determined by ^{13}C-CP/MAS NMR to elucidate drug–PVP interactions and the localized molecular mobility of drug and PVP in the solid dispersions. The chemical shift of the PVP carbonyl carbon increased as the drug content increased, appearing to reach a plateau at a molar ratio of drug to PVP monomer unit of approximately 1:1, suggesting hydrogen bond interactions between the PVP carbonyl group and the drugs. T_1 of the PVP carbonyl carbon in the solid dispersions increased as the drug content increased, indicating that the mobility of the PVP carbonyl carbon was decreased by hydrogen bond interactions. T_1 of the drug carbons increased as the PVP content increased, and this increase in T_1 became less obvious when the molar ratio of PVP monomer unit to drug exceeded approximately 1:1. These results suggest that the localized motion of the PVP pyrrolidone ring and the drug molecules is reduced by hydrogen bond interactions. Decreases in localized mobility appear to be one of the factors that stabilize the amorphous state of drugs.
 J Pharm Sci 95:318–325, 2006
Keywords: spin-lattice relaxation time; amorphous; solid dispersion; stability; molecular mobility

INTRODUCTION

To improve their dissolution rate and solubility, poorly soluble drugs are used in the amorphous form. However, drugs in the amorphous form are generally less stable than crystalline drugs because of their higher energy state and higher molecular mobility. It is well known that poly (vinylpyrrolidone) (PVP) can reduce the crystallization rate of many amorphous drugs.[1–10] This stabilization by PVP is partly attributed to its ability to decrease molecular mobility, as indicated by increases in the glass transition temperature (T_g).[9] Observations of increases in the enthalpy relaxation time of amorphous drugs in the presence of small amounts of PVP also suggest decreases in molecular mobility.[2,7,10] We have reported that the overall crystallization rates of amorphous phenobarbital or nifedipine were reduced by 2–3 orders of magnitude by addition of a small amount of PVP, and that amorphous phenobarbital was stabilized more effectively by PVP than was amorphous nifedipine.[10] The enthalpy relaxation time of amorphous nifedipine increased from 1.2 to 18 days in the presence of 10% PVP, whereas that of amorphous phenobarbital increased from 1.0 to 3.7 days in the presence of 5% PVP. The enthalpy relaxation times of the solid dispersions, however, do not seem to be long

Correspondence to: Yukio Aso (Telephone: +81-3-3700-8547; Fax: +81-3-3707-6950; E-mail: aso@nihs.go.jp)

Journal of Pharmaceutical Sciences, Vol. 95, 318–325 (2006)

enough to explain fully the large increases in stability of the amorphous drugs.

Hydrogen bond interactions between PVP and drugs have been detected by FT–IR,[2,11] FT–Raman[12–15], and water vapor sorption[16,17] measurements, and may be one of the factors involved in stabilization of amorphous drugs by PVP.[2,4–8,11] It is of great interest to elucidate the effects of hydrogen bond interactions on the mobility of drug molecules in amorphous solid dispersions. Shamblin and Zografi studied the effects of hydrogen bond interactions on the molecular mobility of amorphous sucrose by measuring the enthalpy relaxation of amorphous sucrose in the presence of dextran, PVP, poly(vinylpyrrolidone-co-vinyl acetate), or trehalose. Although the T_g values of the sucrose-additive mixtures studied were similar to that of sucrose, the rate of enthalpy relaxation of sucrose was smaller after addition of additives with higher T_g values. The decreased molecular mobility of sucrose was attributed to interactions that led to coupling of the molecular motions of sucrose and of the additives.[18] Measuring the mobilities of drug and additive molecules as a function of additive content may be useful to elucidate the effects of hydrogen bond interactions on molecular mobility. Enthalpy relaxation measurements, however, seem not to be applicable for this purpose, since the T_g of the drug-additive mixtures would change as the additive content increased and comparison of the enthalpy relaxation times of the mixtures would be difficult.

^{13}C-CP/MAS NMR measurements may be particularly useful for such investigations, because knowledge of ^{13}C-NMR spin-lattice relaxation times (T_1) can indicate the molecular mobility of each compound in multi-component systems.[19–22] Hydrogen bond interactions of PVP may also be detected from changes in the chemical shift of the PVP carbonyl carbons, in a similar manner to that of the poly(3-hydroxybutyrate) carbonyl carbon in the presence of polyvinyl alcohol.[23]

In this paper, T_1 and chemical shift values of PVP and drug carbons in nifedipine–PVP and phenobarbital–PVP solid dispersions with various PVP contents were determined by ^{13}C-CP/MAS NMR in order to elucidate the effects of hydrogen bond interactions on the molecular mobility of amorphous nifedipine and phenobarbital. The characteristics of the interaction between nifedipine and PVP were compared with those of the interaction between phenobarbital and PVP to explain the differences in the ability of PVP to stabilize the two drugs.

EXPERIMENTAL

Materials

Nifedipine (melting point 172°C) and PVP (PVP-40, Mw 40000) were purchased from Sigma (St. Louis, MO) and used as received. Phenobarbital was prepared from sodium phenobarbital (Wako Pure Chemical Ind., Osaka, Japan) according to a previously described method.[24] Shortly, phenobarbital was precipitated from aqueous sodium phenobarbital solution by neutralization. The precipitate obtained was then crystallized from acetone solution. The melting point of the crystalline phenobarbital was observed at 175°C by DSC, consistent with that reported previously.[24] The peak area of the crystalline phenobarbital in high performance liquid chromatogram was confirmed to be equivalent to that of sodium phenobarbital.

Preparation of Nifedipine–PVP and Phenobarbital–PVP Solid Dispersions

Nifedipine–PVP and phenobarbital–PVP solid dispersions were prepared by melting and subsequent rapid cooling of mixtures of each drug and PVP. Nifedipine or phenobarbital were dissolved in methanol with PVP at various weight ratios. The methanol was then evaporated off with a rotary evaporator under reduced pressure. The mixture thus obtained was ground in a mortar and then dried in a vacuum chamber at about 60°C for 1 day. The dried mixtures were heated at approximately 180°C for 10–20 min in a Teflon vessel and then were cooled by immersion in liquid nitrogen. The amorphous nature of each sample was confirmed by glass transition temperature (T_g) measurements and observation under polarized light. T_g measurements were carried out using a 2920 differential scanning calorimeter (DSC) and the refrigerator cooling system (TA instrument, New Castle, DE). The modulated temperature program used was ±0.5°C modulation amplitude within 100 s and an underlying heating rate of 1°C/min. Hermetic aluminum sample pans were used for measurement. Temperature and cell constant calibration of the instrument was carried out using indium. DSC cell was purged by dry nitrogen (30 mL/min). Table 1 shows the T_g of nifedipine– and phenobarbital–PVP solid dispersions. Single glass transition temperature was observed for all the samples studied, indicating that the dispersions were amorphous.

Table 1. T_g of Nifedipine–PVP and Phenobarbital–PVP Solid Dispersions

	T_g (°C)[a]
Nifedipine	41.9 ± 0.4
Nifedipine–PVP 90:10	43.5 ± 1.0
Nifedipine–PVP 80:20	51.9 ± 0.1
Nifedipine–PVP 70:30	69.5 ± 0.8
Nifedipine–PVP 50:50	96.9 ± 0.4
Nifedipine–PVP 30:70	124.9 ± 0.7
Phenobarbital	40.8 ± 0.2
Phenobarbital–PVP 90:10	46.5 ± 0.1
Phenobarbital–PVP 80:20	57.7 ± 0.2
Phenobarbital–PVP 65:35	89.6 ± 0.5
Phenobarbital–PVP 50:50	115.3 ± 0.9
Phenobarbital–PVP 70:30	135.5 ± 0.6
PVP	168.2 ± 0.6

[a]Average and standard deviation of the mid-point T_g ($n = 3$).

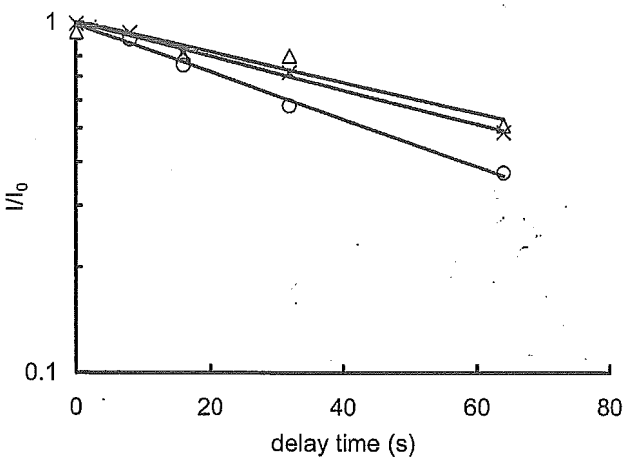

Figure 1. Typical signal decay of the PVP carbonyl carbon. ○, pure PVP; △, nifedipine–PVP (8:2); ×, phenobarbital–PVP (8:2).

^{13}C High-Resolution Solid State NMR

NMR measurements were carried out using freshly prepared samples in order to minimize the possible effect of enthalpy relaxation on the T_1. The amorphous samples obtained were very gently pulverized by using a spatula and, avoiding mechanical stress, put into NMR rotors. The NMR sample preparation was carried out in a grove bag filled with dry nitrogen in order to avoid water sorption by samples. The water content of the samples was determined to be less than 0.1 w/w% by the Karl–Fisher method. NMR measurements were carried out at 27°C with a Varian Unity plus spectrometer (Varian, Inc., Palo Alto, CA) at a proton resonance frequency of 400 MHz. The chemical shift calibration of the instrument was conducted with hexamethylbenzene (methyl group at 17.3 ppm) as an external standard. The pulse sequence for T_1 measurement was that reported by Torchia.[25] The spinning rate was 6.5 kHz, the contact time was 1 ms, delay time was 0.1, 8, 16, 32, 64 s, and recycling delay was 5 s. Scans (400–500) were accumulated for each spectrum. Signals were assigned according to chemical shift data reported for PVP, nicardipine, nimodipine, nifedipine, and phenobarbital glucoside.[19,26–30] Nifedipine carbons observed at 103 ppm were assigned to be C-2 and C-6 carbons[26,27] or C-3 and C-5 carbons.[29] Figure 1 shows the typical signal decay of the PVP carbonyl carbon. When the PVP carbonyl group interacts with drugs, signal decay is expected to be describable by the sum of two or more exponential functions, since there are at least two types of PVP carbonyl carbons with different molecular mobilities. It was, however, difficult to separate the signal decay into two exponential functions, since differences in T_1 were small, as shown in Figure 1. Therefore, the signal decay of all carbons was described by a single exponential function and apparent T_1 values were reported in this paper. There was no significant change in DSC thermograms, suggesting no crystallization occurring in the solid dispersion samples after NMR measurements.

RESULTS AND DISCUSSION

Effect of Drug Content on Chemical Shift and T_1 of PVP Carbons

Figures 2 and 3 show typical ^{13}C-CP/MAS NMR spectra of nifedipine–PVP and phenobarbital–PVP solid dispersions. The chemical shift of the PVP carbonyl carbon, observed at approximately 175 ppm, increased in the presence of nifedipine or phenobarbital. For the phenobarbital–PVP solid dispersion, the chemical shift of C-2 carbon of PVP decreased from 19.5 ± 0.1 ppm to 19.0 ± 0.2 ppm. In contrast, the chemical shift of PVP carbons other than the carbonyl carbon did not change within experimental error for the nifedipine–PVP solid dispersions. Figure 4 shows the effects of drug content on the chemical shift of the PVP carbonyl carbon. The chemical shift

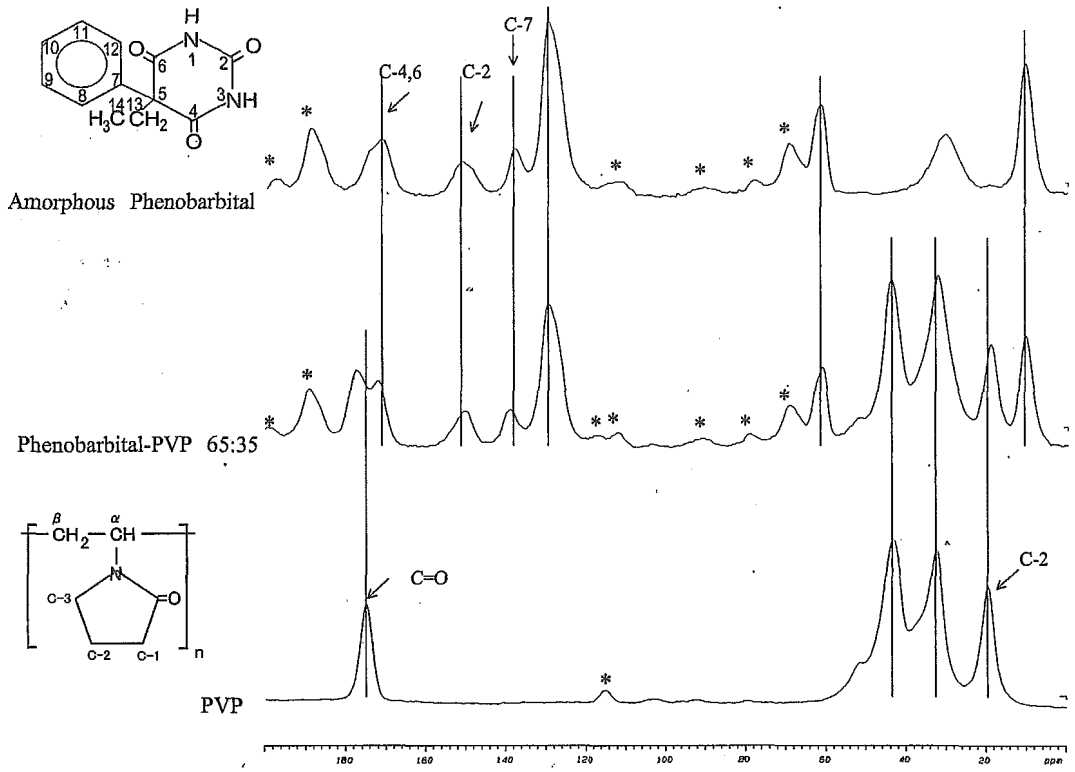

Figure 2. Typical ^{13}C CP/MAS spectra of amorphous phenobarbital–PVP. * represents spining side bands.

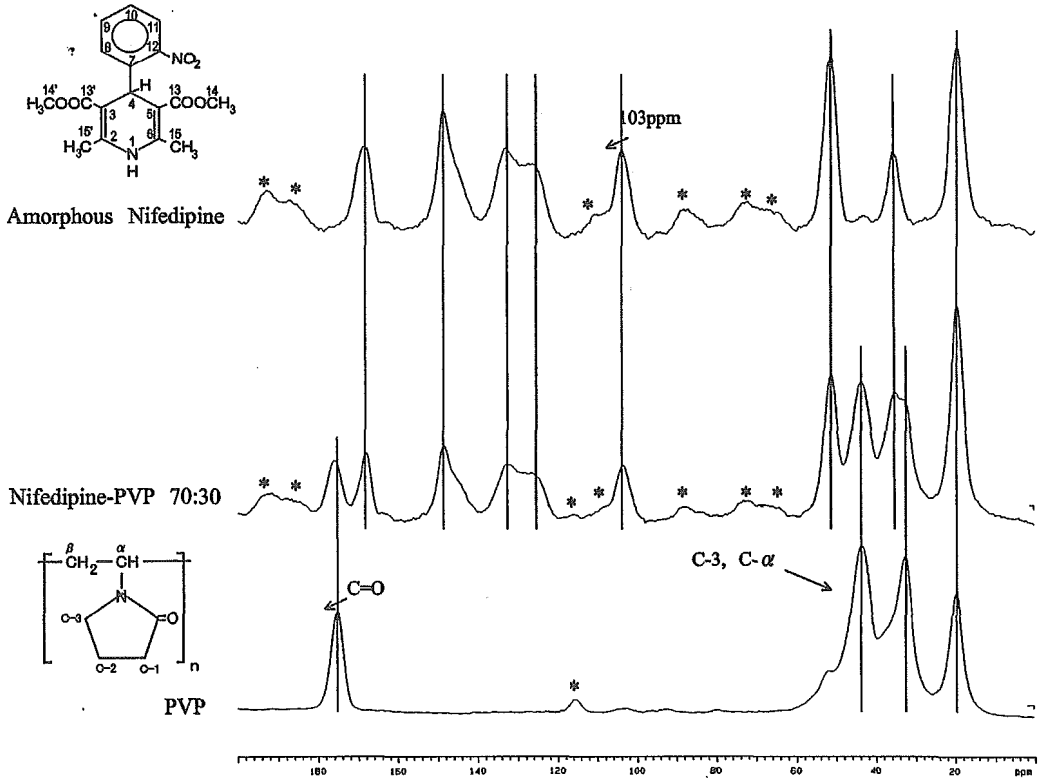

Figure 3. Typical ^{13}C CP/MAS spectra of amorphous nifedipine–PVP. * represents spining side bands.

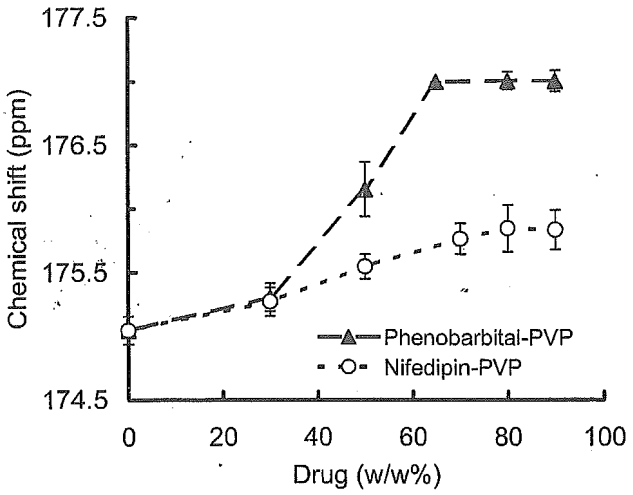

Figure 4. Effect of phenobarbital and nifedipine on the chemical shift of the PVP carbonyl carbon. Error bars represent standard deviation ($n = 3$).

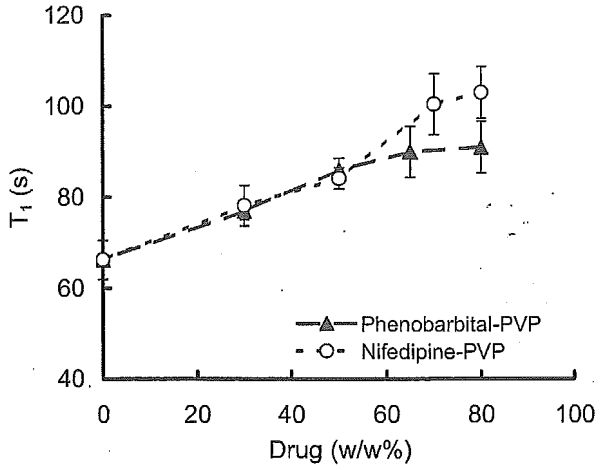

Figure 5. Effect of phenobarbital and nifedipine on the T_1 of the PVP carbonyl carbon. Error bars represent standard deviation ($n = 3$).

increased as the drug content increased and appeared to reach a plateau at a nifedipine content of approximately 70 w/w% or a phenobarbital content of approximately 65 w/w%. These drug contents correspond to a molar ratio of drug to PVP monomer unit of 1:1. The increases in the chemical shift of PVP carbon (more than 1 ppm) was larger than those observed for other PVP carbons (less than 0.5 ppm). It has been reported that the chemical shift of the carbonyl carbon of poly(3-hydroxybutyrate) (PHB) increases by approximately 1 ppm in the presence of polyvinyl alcohol (PVA), indicating changes in the electronic environment of the carbonyl carbon resulting from hydrogen bonding between the carbonyl group of PHB and the hydroxyl group of PVA.[23] Further, hydrogen bond interaction between the PVP carbonyl group and the nifedipine NH group has been indicated by FT–IR spectroscopy.[11] Therefore, the increases in chemical shift of the PVP carbonyl carbon observed in this study suggests hydrogen bond interactions between the PVP carbonyl group and a hydrogen donor group (NH group) from the drug, in a similar manner to the PHB-PVA systems.

Figure 5 shows the effects of drug content on the T_1 of the PVP carbonyl carbon in the pyrrolidone ring. As the drug content increased, T_1 in the slow motional regime increased, indicating that the mobility of the PVP carbonyl carbon decreased. The T_g values of nifedipine–PVP and phenobarbital–PVP solid dispersions decreased as the drug content increased (Tab. 1), indicating that the molecular mobility of the matrices increased with drug content. These findings suggest that T_1 does not reflect the global motion of the PVP–drug matrix but rather the localized motion of the PVP pyrrolidone ring. The decreased local mobility of the pyrrolidone ring was supported by changes in the T_1 of the C-2 carbon of the pyrrolidone ring. Figure 6 shows the effect of phenobarbital on the T_1 of the C-2 carbon of the pyrrolidone ring. The T_1 value increased in a similar manner to that of the PVP carbonyl carbon shown in Figure 5. The signals of the C-3 and C-α carbons of PVP overlap

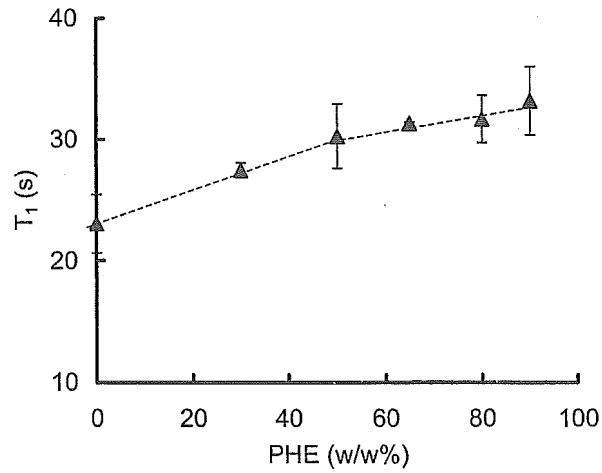

Figure 6. Effect of phenobarbital content on the T_1 of the PVP C-2 carbon in phenobarbital–PVP. Error bars represent standard deviation ($n = 3$).

each other and are observed at 45 ppm. The apparent T_1 of these carbon atoms increased in the presence of nifedipine and phenobarbital in a similar manner to that of the PVP carbonyl carbon (data not shown). Although the C-2 and C-3 carbons are not considered to interact directly with phenobarbital or nifedipine, the interaction of the PVP carbonyl carbon may decrease the motion of all the carbon atoms in the pyrrolidone ring. In summary, hydrogen bond interactions between PVP and the drugs appeared to affect the chemical shift of the PVP carbonyl carbon as well as the T_1 values of the carbonyl, C-2 and C-3 carbons of PVP. Changes in the T_1 value seem to be a more useful measure than chemical shift for detecting PVP–drug interactions, since changes in T_1 were larger than those in chemical shift.

Effect of PVP Content on the T_1 Values of Drug Carbons

Figure 7 shows the effect of PVP content on the T_1 of the phenobarbital C-2, C-4, C-5, and C-6 carbons. The T_1 values of these carbons increased as the PVP content increased. This increase in T_1 became less obvious at PVP contents greater than approximately 35 w/w%, corresponding to a molar ratio of phenobarbital to PVP monomer unit of 1:1. The T_1 values of these carbons increased by 1.5–2 times in the presence of PVP. The order of the relative change in the T_1 values was C-4,6 > C-5>C-2. Although larger change in T_1 values was expected for carbons near the NH group, there was no clear tendency between the relative change in the T_1 values and the proximity of the carbons to the NH group. Hydrogen bond interaction may equally affect the mobility of these carbons, since these carbons comprise the primidinetrione ring. Increased T_1 values after addition of PVP were also observed for nifedipine carbons observed at 103 ppm, as shown in Figure 8. The T_1 values increased as the PVP content increased, in a similar manner to that observed for phenobarbital–PVP solid dispersions. This finding suggests that the localized motion of the drugs decreased as a result of hydrogen bond interactions between PVP and the drugs. This is consistent with the results obtained for PVP carbons described above. PVP affected the T_1 of phenobarbital C-2, C-4, C-5, and C-6 carbons and the T_1 of nifedipine carbons observed at 103 ppm. This may be due to the differences in the interaction site of the drugs; in contrast to nifedipine having one NH group, phenobarbital has two NH groups that can interact with PVP carbonyl. The fact suggests that PVP may decrease the localized motion of phenobarbital more effectively than it does that of nifedipine. The difference in the ability of PVP to decrease the localized motion of the two drugs may explain the difference in the ability of PVP to stabilize amorphous phenobarbital and nifedipine; the overall crystallization rate of amorphous phenobarbital was reduced by 2–3 orders of magnitude by 5 w/w% PVP, whereas 10 w/w% PVP was required to

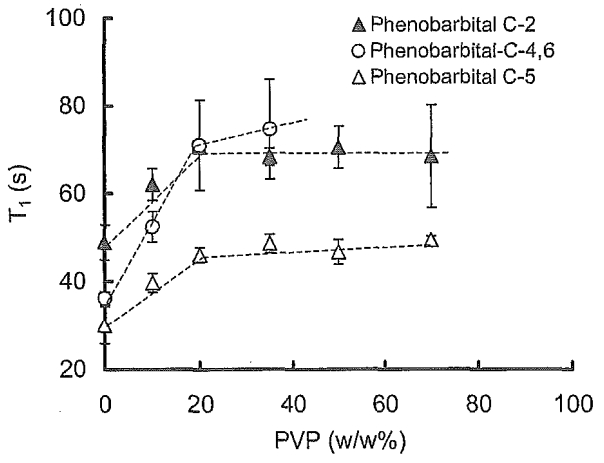

Figure 7. Effect of PVP on the T_1 of phenobarbital carbons. Error bars represent standard deviation ($n = 3$).

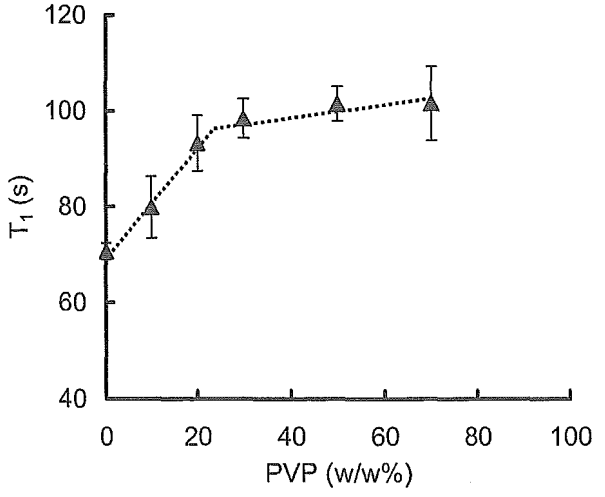

Figure 8. Effect of PVP on the T_1 of nifedipine carbons at 103 ppm (C-2, C-6). Error bars represent standard deviation ($n = 3$).

achieve a similar effect with nifedipine.[10] Therefore, inhibition of the localized motion of drugs appears to be one of the mechanisms by which PVP stabilizes the amorphous state.

CONCLUSION

Changes in the chemical shift of the PVP carbonyl carbon suggest the occurrence of hydrogen bond interactions between the PVP carbonyl group and nifedipine or phenobarbital. These interactions increased the T_1 values of the carbon atoms of PVP and the drugs, suggesting that the localized molecular motion of the drugs was decreased. This decreased molecular mobility appears to be one of the factors that stabilize the amorphous state of drugs.

ACKNOWLEDGMENTS

A part of this work was supported by a Grant-in-aid for Research on Health Sciences Focusing on Drug Innovation from The Japan Health Sciences Foundation.

REFERENCES

1. Yoshioka M, Hancock BC, Zografi G. 1995. Inhibition of indomethacin crystallization in Poly(vinylpyrrolidone) coprecipitate. J Pharm Sci 84:983–986.
2. Matsumoto T, Zografi G. 1999. Physical properties of solid molecular dispersions of indomethacin with poly(vinylpyrrolidone) and poly(vinylpyrrolidone-co-vinyl-acetate) in relation to indomethacin crystallization. Pharm Res 16:1722–1728.
3. Crowley KJ, Zografi G. 2003. The effect of low concentrations of molecularly dispersed poly(vinylpyrrolidone) on indomethacin crystallization from the amorphous state. Pharm Res 20:1417–1422.
4. Shamblin SL, Huang EY, Zografi G. 1996. The effects of co-lyophilized polymer additives on the glass transition temperature and crystallization of amorphous sucrose. J Thermal Anal 47:1567–1579.
5. Shamblin SL, Zografi G. 1999. The effect of absorbed water on the properties of amorphous mixtures containing sucrose. Pharm Res 16:1119–1124.
6. Zeng XM, Martin GP, Marriott C. 2000. Effects of molecular weight of polyvinylpyrrolidone on the glass transition temperature and crystallization of co-lyophilized sucrose. Int J Pharm 218:63–73.
7. Miyazaki T, Yoshioka S, Aso Y, Kojima S. 2004. Ability of polyvinylpyrrolidone and polyacrylic acid to inhibit the crystallization of amorphous acetaminophen. J Pharm Sci 93:2710–2717.
8. Khougaz K, Clas S. 2000. Crystallization inhibition in solid dispersions of MK-0591 and poly(vinylpyrrolidone) polymer. J Pharm Sci 89:1325–1334.
9. Berggren J, Alderborn G. 2004. Long-term stabilization potential of poly(vinylpyrrolidone) for amorphous lactose in spray-dried composites. Eur J Pharm Sci 21:209–215.
10. Aso Y, Yoshioka S, Kojima S. 2004. Molecular mobility-based estimation of the crystallization rates of amorphous nifedipine and phenobarbital in poly(vinylpyrrolidone) solid dispersions. J Pharm Sci 93:384–391.
11. Foster A, Hempennstall J, Rades T. 2001. Characterization of glass solutions of poorly water-soluble drugs produced by melt extrusion with hydrophilic amorpous polymers. J Pharm Pharmacol 53:303–315.
12. Taylor LS, Zografi G. 1997. Spectroscopic characterization of interactions between PVP and indomethacin in amorphous molecular dispersions. Pharm Res 14:1691–1698.
13. Shamblin SS, Taylor LS, Zografi G. 1998. Mixing tendencies of co-lyophilized sucrose-additive systems. J Pharm Sci 87:694–701.
14. Taylor LS, Zografi G. 1998. Sugar-polymer hydrogen bond interactions in lyophilized mixtures. J Pharm Sci 87:1615–1621.
15. Taylor LS, Langkilde FW, Zografi G. 2001. Fourier transform Raman spectroscopic study of the interaction of water vapor with amorphous polymers. J Pharm Sci 90:888–901.
16. Zhang J, Zografi G. 2001. Water vapor absorption into amorphous sucrose-poly (vinylpyrrolidone) and trehalose-poly(vinylpyrrolidone) mixtures. J Pharm Sci 90:1375–1385.
17. Crowly KJ, Zografi G. 2002. Water vapor sorption into amorphous hydrophobic drug/poly(vinylpyrrolidode) dispersions J Pharm Sci 91:2150–2165.
18. Shamblin SL, Zografi G. 1998. Enthalpy relaxation in binary amorphous mixtures containing sucrose. Pharm Res 15:1828–1834.
19. Oksanen CA, Zografi G. 1993. Molecular mobility in mixtures of absorbed water and solid poly(vinylpyrrolidone). Pharm Res 10:791–799.
20. Yoshioka S, Aso Y, Kojima S, Sakurai S, Fujiwara T, Akutsu H. 1999. Molecular mobility of protein lyophilized formulations linked to the molecular mobility of polymer excipients as determined by high resolution ^{13}C solid-state NMR. Pharm Res 16:1621–1625.
21. Aso Y, Sumie Yoshioka S, Zhang J, Zografi G. 2002. Effect of water on the molecular mobility of sucrose and PVP in a colyophilized formulation as measured by ^{13}C–NMR relaxation time. Chem Pharm Bull 50:822–826.

22. Yoshioka S, Aso Y, Kojima S. 2003. Molecular mobility of lyophilized poly(vinylpyrrolidone) and methyl cellulose as determined by the laboratory and rotating frame spin-lattice relaxation time of ^{1}H and ^{13}C. Chem Pharm Bull 51:1289–1292.
23. Yoshie N, Azuma Y, Sakurai M, Inoue Y. 1995. Crystallization and compatibility of poly(vinyl alcohol)/poly(3-hydroxybutyrate) blends: Influence of blend composition and tacticity of poly(vinyl alcohol). J Apply Polym Sci 56:17–24.
24. Kato Y, Watanabe F. 1978. Relationship between polymorphism and bioavailability of phenobarbital. Yakugaku Zasshi 98:639–648.
25. Torchia DA. 1978. The measurement of proton-enhanced carbon–13 T_1 values by a method that suppresses artifacts. J Magn Reson 30:613–618.
26. Yokota K, Abe A, Hosaka S, Sakai I, Saito H. 1978. A ^{13}C nuclear magnetic resonance study of covalently cross-linked gels. Effect of chemical composition, degree of cross-linking, and temperature to chain mobility. Macromolecules 11:95–100.
27. Gaggelli E, Marchettini N, Valensin G. 1987. Nuclear magnetic resonance investigations of calcium-antagonist drugs. Part1. Conformational and dynamic features of nimodipine {3-[(2-methoxyethoxy)carbonyl]-5-(isopropoxycarbonyl)-4-(3-nitrophenyl)-2,6-dimethyl-1,4-dihydropyridine} in [$^{1}H_6$] dimethyl sulphoxide. J Chem Soc Perkin Trans II 1987:1707–1711.
28. Kovesdi I, Kapiller-Dezsofi R. 1996. NMR investigation of nifedipine. Acta Pharm Hung 66:11–14.
29. Soine WH, Soine PJ, England TM, Overton BW, Merat S. 1989. Synthesis of N-β-D-glucopyranosyl derivatives of barbital, phenobarbital, metharbital, and mephobarbital. Carbohydrate Res 19:105–113.
30. Belciug MP, Ananthanarayanan VS. 1994. Interaction of calcium channel antagonists with calcium: Structural studies on nicardipine and its Ca^{2+} complex. J Med Chem 37:4392–4399.

JPS/05-319(20504)

Negligible Contribution of Molecular Mobility to the Degradation Rate of Insulin Lyophilized with Poly(vinylpyrrolidone)

SUMIE YOSHIOKA, YUKIO ASO, TAMAKI MIYAZAKI

National Institute of Health Sciences, 1-18-1 Kamiyoga, Setagaya-ku, Tokyo 158-8501, Japan

Received 1 January 2005; revised 15 April 2005; accepted 25 September 2005

Published online ? ? ? ? in Wiley InterScience (www.interscience.wiley.com). DOI 10.1002/jps.20504

ABSTRACT: The purpose of this study is to confirm the speculation which arose in our previous study that the degradation rate of insulin lyophilized with poly(vinylpyrrolidone) (PVP) is mainly governed by the chemical activational barrier rather than molecular mobility. This speculation was based on the degradation data of insulin lyophilized with poly(vinylpyrrolidone) K-30 (PVP K-30), which was obtained at temperatures well below the glass transition temperature (T_g). In this study, the degradation rate of insulin at temperatures below and above T_g was determined using PVP 10k as an excipient, instead of PVP K-30, in order to examine whether or not the temperature dependence of the degradation rate changes around T_g. The relative contributions of molecular mobility and the activational barrier, calculated from the temperature- and T_g-dependence of the degradation rate, indicated that the contribution of molecular mobility to the degradation rate was negligible. Furthermore, the negligible contribution of molecular mobility was confirmed by the lack of significant change observed in the temperature- and T_g-dependence of the rate around T_g. J Pharm Sci 9999:1–5, 2006

Keywords: solid-state stability; glass transition; lyophilization; amorphous; physicochemical; molecular mobility; insulin

INTRODUCTION

An understanding of how the chemical stability of solid formulations is affected by molecular mobility is beneficial in the development and evaluation of stable solid dosage forms. We recently proposed an equation for quantitatively assessing the contribution of molecular mobility to the chemical reactivity of amorphous solids (Eq. 1),[1]

$$k' = k\left(\frac{\alpha D_r}{k + \alpha D_r}\right) = k\left(\frac{\alpha T\left(\frac{1}{\tau}\right)^{\xi}}{k + \alpha T\left(\frac{1}{\tau}\right)^{\xi}}\right) \quad (1)$$

where k' is the rate constant for a reaction in which the rate-determining step involves molecular diffusion.[2] k is the rate constant at the condition under which reactants have high diffusibility, such that k may be described by Eq. 2 using the activation energy (ΔH), the frequency factor (A) and the gas constant (R).

$$k = A \exp\left(\frac{-\Delta H}{RT}\right) \quad (2)$$

D_r is diffusion coefficient of the reactant and α is a constant representing the correlation between D_r and reaction rate. D_r was assumed to relate to the structural relaxation time (τ) according to Eq. 3,

$$\frac{D_{r2}}{D_{r1}} \approx \left(\frac{T_2}{T_1}\right)\left(\frac{\tau_1}{\tau_2}\right)^{\xi} \quad (3)$$

where ξ is a constant that represents the degree of decoupling between D_r and τ.[3] k' in Eq. 1 can be converted to t_{90} (time required for 10%

Correspondence to: Sumie Yoshioka (Telephone: 81-3-3700-8547; Fax: 81-3-3707-6950; E-mail: yoshioka@nihs.go.jp)

Journal of Pharmaceutical Sciences, Vol. 9999, 1–5 (2006)

degradation) according to Eq. 4 for first-order degradation.

$$k' = \frac{-\ln(0.9)}{t_{90}} \quad (4)$$

Using Eq. 1, the relative contribution of molecular mobility and that of the chemical activational barrier, reflected in the activation energy, were calculated for the chemical degradation of insulin lyophilized with trehalose or poly(vinylpyrrolidone) K-30 (PVP K-30).[1] For the insulin-trehalose system, the ratio of the observed rate constant (k') to the rate constant governed only by the chemical activational barrier (k) at the glass transition temperature (T_g) was 0.05 at 12% relative humidity (RH). This ratio (k'/k) was greater than 0.9 at humidity levels between 23%RH and 60%RH, indicating that the significance of molecular mobility as a determinant for reactivity is greater at lower humidity. The insulin-PVP K-30 system, in contrast, exhibited a k'/k value greater than 0.95 even at 12%RH, suggesting that the significance of molecular mobility is small. This speculation was based on the degradation data obtained at temperatures well below T_g, but not on the observation that the temperature dependence of k' does not significantly change around T_g. This is because k' values around T_g could not be determined because of the high T_g of the insulin-PVP K-30 system.

In this study, the degradation rate of insulin lyophilized with PVP 10k was determined as a function of temperature and humidity. The insulin-PVP 10k system has a T_g value lower than that of the insulin-PVP K-30 system, such that the degradation rate can be determined at temperatures below and above T_g, allowing us to examine whether the temperature dependence of the rate changes around T_g. The temperature- and T_g-dependence of the degradation rate was analyzed to obtain the relative contributions of molecular mobility and the activational barrier.

EXPERIMENTAL

Lyophilization of Insulin

Lyophilization was carried out in a similar manner as reported previously.[1] Human zinc insulin (Humulin® RU-100, Eli Lilly & Co.[Q2]) was converted into the zinc-free neutral form by dialysis. PVP 10k (average molecular weight of 10k, Sigma Chemical Co.[Q3]) was added to the solution to make a 5 mg/mL of PVP 10k solution and pH was adjusted to 4.0. The ratio of insulin to PVP 10k was 1:1.5 w/w. Four hundred microliters of the solution were frozen in a polypropylene sample tube (10 mm diameter), and then dried at a vacuum level below 5 Pa for 23.5 h in a lyophilizer (Freezevac C-1, Tozai Tsusho Co., Tokyo). The shelf temperature was between −35 and −30°C for the first 1 h, 20°C for the subsequent 19 h, and 30°C for the last 3.5 h.

Lyophilized samples were stored at 15°C for 24 h in a desiccator with a saturated solution of LiCl H_2O (12%RH), potassium acetate (23%RH), K_2CO_3 $2H_2O$ (43%RH), or NaBr $2H_2O$ (60%RH) to obtain samples with various T_g values.

Determination of T_g by Differential Scanning Calorimetry (DSC)

Modulated temperature DSC experiments were performed using a commercial system (2920; TA Instruments, DE) attached to a refrigerated cooling accessory. The conditions were as follows: modulation period of 100 s, a modulation amplitude of ±0.5°C, and an underlying heating rate of 1°C/min. Samples were put in a hermetic pan. Temperature calibration was performed using indium. The samples, pre-equilibrated at 12%RH, 23%RH, 43%RH, and 60%RH, exhibited a T_g value of 116°C, 88°C, 65°C, and 46°C, respectively. A representative DSC scan is shown in Figure 1. Change in heat flow corresponding to the T_g of PVP 10k alone was not observed, indicating no significant phase separation.

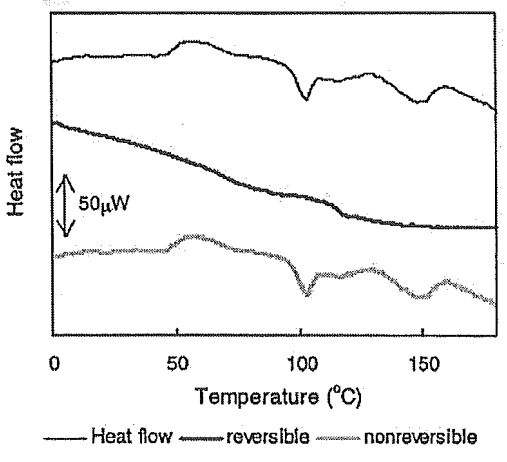

Figure 1. Modulated DSC scan for insulin lyophilized with PVP 10k (12%RH).

DOI 10.1002/jps

Measurement of Insulin Degradation by HPLC and High-Performance Size-Exclusion Chromatography (HP-SEC)

Lyophilized samples with various T_g values in tubes with a tight screw-cap were stored at a constant temperature (20–90°C), removed at various times, and stored in liquid nitrogen until assayed. Samples were dissolved in 1.5 mL of 0.01 M $(NH_4)_2SO_4$ (pH 2.2, adjusted with concentrated H_2SO_4) and each 20 μL aliquot of the solution (insulin concentration was 0.9 mg/mL) was subjected to reverse phase HPLC (RP-HPLC) and high-performance size-exclusion chromatography (HP-SEC), respectively.

The concentration of intact insulin was quantified using a modular RP-HPLC, as reported previously.[1] The column used was Inertsil WP-300 (C8, 4.6 mm × 250 mm, GL Science Inc.[Q4]) maintained at 35°C. Elutions were performed using a mixture of 0.01 M $(NH_4)_2SO_4$ (pH 2.2) and acetonitrile solution of 0.07% (v/v) trifluoroacetic acid (72.5:27.5) for 1 min. The ratio of the acetonitrile solution increased linearly from 27.5% to 30% in 15 min, 30% to 35% in 22 min. The detection wavelength was 214 nm.

The amount of insulin monomers was determined by a HP-SEC, as reported previously.[1] The column used was Protein-Pak 125 (7.8 mm × 300 mm, Waters) maintained at 25°C. A 2.5 M acetic acid solution containing 4 mM L-arginine and 4% (v/v) acetonitrile was eluted at a rate of 1 mL/min. The chaotropic power of the mobile phase was assumed to be sufficient to disrupt all non-covalent interactions, so that covalent transamidation or other covalent bonding of insulin monomers to form dimer can be detected by the SEC.

RESULTS AND DISCUSSION

Figure 2 shows the time courses of insulin degradation in the insulin-PVP 10k system at 60%RH, determined by HPLC. Similar time courses were obtained at 12%RH, 23%RH, and 43%RH. Degradation in the initial stage was describable with first-order kinetics under all the temperature and humidity conditions studied, although the empirical Kohlrausch–Williams–Watts (KWW) equation (Eq. 5) could better fit the data exhibiting more than 10% degradation ($\beta_{KWW} = 0.5$). t_{90} was calculated from the apparent first-order constant in the initial stage according to Eq. 4. The time course for the amount

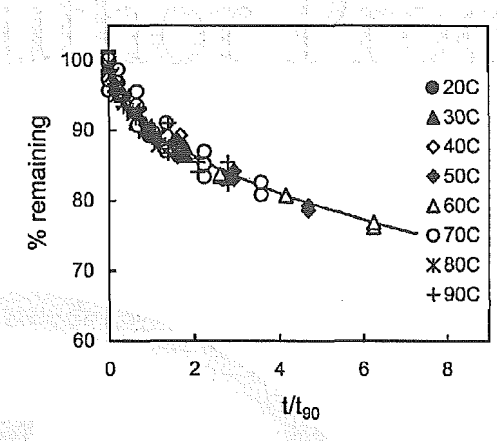

Figure 2. Time courses of insulin degradation at 60%RH and various temperatures measured by HPLC. Solid line represents the regression line obtained according to the KWW equation with a β_{KWW} value of 0.5.

of insulin monomers in the initial stage, determined by HP-SEC, was also describable with first-order kinetics under all the temperature and humidity conditions studied (data not shown).

$$\phi(t) = \exp\left[-\left(\frac{t}{\tau_{KWW}}\right)^{\beta_{KWW}}\right] \quad (5)$$

Figure 3 compares the t_{90} at 12%RH and 60%RH determined by HPLC with that determined by HP-SEC. The HPLC-derived t_{90} was significantly smaller than the SEC-derived t_{90} at 12%RH, whereas the difference was not significant at 60%RH. The t_{90} obtained at 23%RH and 43%RH (data not shown) indicated that the difference between HPLC-derived t_{90} and the SEC-derived

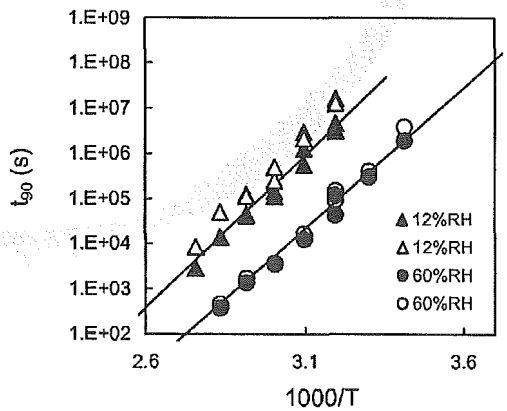

Figure 3. Comparison of t_{90} determined by HPLC (closed symbol) and that determined by HP-SEC (open symbol).

t_{90} became less conspicuous as humidity increased. It has been observed that the major degradation pathways of insulin in acidic solution[4] and in lyophilized solids derived from acidic solutions[5] are A21-desamido insulin formation and dimerization via the cyclic anhydride intermediate. The same degradation pathways were observed in the insulin-PVP 10k system studied. A21-desamido insulin was identified based on the HPLC retention time coincident with that of the A21-desamido insulin prepared by the method reported.[6] Insulin dimer was detected by SEC. Formation of A21-desamido insulin, which reduces the HPLC insulin peak but not the SEC insulin peak, as well as insulin dimer formation can explain the SEC-derived t_{90} longer than the HPLC-derived t_{90}. The increase in the difference between the HPLC-derived t_{90} and the SEC-derived t_{90} with decreasing humidity is attributable to the decrease in molecular mobility that results in suppression of dimer formation.[5]

Figure 4 shows the temperature- and T_g-dependence of t_{90} obtained in the temperature range 20°C–90°C and the humidity range 12%RH–60%RH. The relative contributions to insulin degradation of molecular mobility and the chemical activational barrier were calculated by curve-fitting of the temperature- and T_g-dependence of the observed t_{90} to Eqs. 1 and 4. Solid lines in the figure represent the regression curves obtained. The value of k'/k was estimated to be unity (i.e., the value in parentheses in Eq. 1 was equal to unity), indicating that the significance of molecular mobility as a determinant for the reaction rate was small. As shown in Figure 4A, the t_{90} versus $1/T$ plots were not coincident for different humidity conditions, regardless of the negligible effect of molecular mobility. This finding suggests that ΔH varies with humidity. Curve-fitting provided ΔH estimates of 30.9, 30.5, 29.4, and 28.5 kcal/mol for 12%RH, 23%RH, 43%RH, and 60%RH, respectively, as well as A estimate of 10^{14}/s. Our previous paper[1] reported that ΔH for insulin degradation in insulin-PVP K-30 systems was estimated approximately 20 kcal/mol at 12%RH and 43%RH. However, recalculation after the removal of low-temperature data with large variations yielded ΔH estimates of approximately 30 kcal/mol, which almost consisted with the ΔH estimated for insulin degradation in the insulin-PVP 10k system. This suggests that insulin degradation in the insulin-PVP K-30 system is due to A21-desamido formation and dimerization via the cyclic anhydride intermediate, similarly as in the insulin-PVP 10k system, rather than PVP-insulin adduct formation as speculated from the biased ΔH estimates in the previous paper.

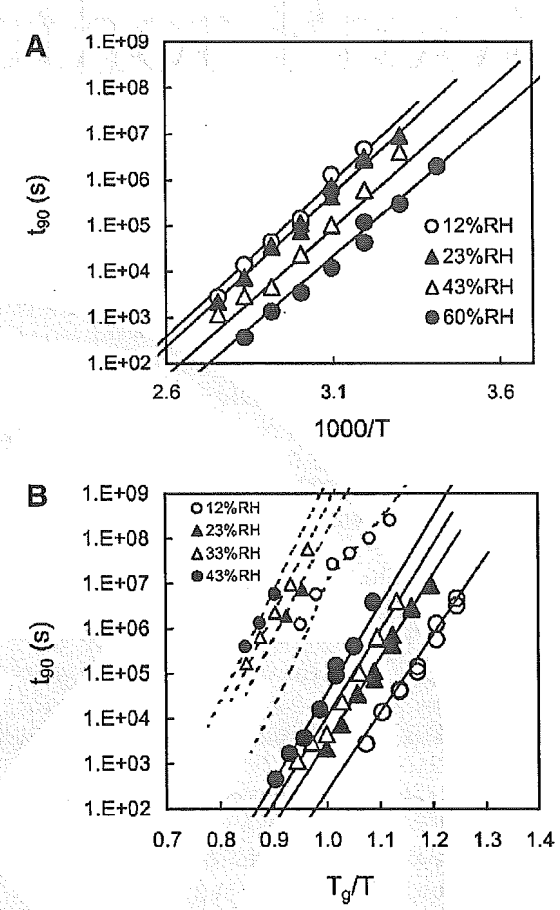

Figure 4. t_{90} of insulin degradation determined by HPLC plotted against $1/T$ (A) and T_g/T (B). Solid lines represent the regression lines obtained according to the Eq. 1. B: Further shows the t_{90} of degradation of insulin lyophilized with trehalose (small symbols and dotted lines), reported previously.[1]

The t_{90} versus T_g/T plots shown in Figure 4B exhibited no change in slope around T_g. Furthermore, the plots for different humidity conditions did not converge around T_g in a manner as expected when molecular mobility is a determinant for degradation rate (as shown in the previous simulation study[1]). These findings indicate that molecular mobility is not a significant determinant for the degradation rate of insulin in the insulin-PVP 10k, as similarly observed in the insulin-PVP K-30 system. Thus, the speculation given rise to in the previous study,[1] that degradation rate is mainly governed by the chemical activational barrier rather than molecular mobility, was confirmed.

DOI 10.1002/jps

Figure 4B compares the temperature- and T_g-dependence of t_{90} for the insulin-PVP 10k system with that of the insulin-trehalose system reported previously.[1] The insulin-trehalose system exhibited a k'/k value (at T_g) larger than 0.9 at humidity levels above 23%RH and a k'/k value (at T_g) of 0.05 at 12%RH, indicating that molecular mobility is a major factor that determines the degradation rate at low humidity. In contrast, molecular mobility was found not to be a determinant for degradation rate in both the insulin-PVP 10k and insulin-PVP K-30 systems even at low humidity. The previous study[1] estimated ΔH of approximately 30 kcal/mol for insulin degradation in the insulin-trehalose systems at 23%RH, 33%RH, and 43%RH, which was close to the ΔH values estimated for degradation in the insulin-PVP 10k and K-30 systems. This finding suggests that the mechanisms for insulin degradation in the insulin-trehalose system is similar to that in the insulin-PVP 10k and K-30 systems (i.e., A21-desamido formation and dimerization via the cyclic anhydride intermediate). Further studies are required to explain why molecular mobility at 12%RH was lowered so as to become the rate-limiting step of the degradation pathway in the insulin-trehalose system, but not in the insulin-PVP 10k and K-30 systems. Interaction between proteins and sugars, which has been demonstrated by many studies, may be a possible explanation.

CONCLUSION

The temperature- and T_g-dependence of the degradation rate of insulin lyophilized with PVP 10k was analyzed by Eqs. 1 and 4 to obtain the relative contributions of molecular mobility and the chemical activational barrier. The results obtained at temperatures below and above T_g confirmed the speculation given rise to in our previous study that insulin degradation in the presence of PVP is mainly governed by the chemical activational barrier rather than molecular mobility.

REFERENCES

1. Yoshioka S, Aso Y. 2005. A quantitative assessment of the significance of molecular mobility as a determinant for the stability of lyophilized insulin formulations. Pharm Res 22: in press[Q5].
2. Karel M, Saguy I. 1991. Effects of water on diffusion in food systems. Adv Exp Med Biol 302: 157–173.
3. Guo Y, Byrn SR, Zografi G. 2000. Physical characteristics and chemical degradation of amorphous quinapril hydrochloride. J Pharm Sci 89: 128–143.
4. Darrington RT, Anderson BD. 1995. Effect of insulin concentration and self-association on the partitioning of it's a-21 cyclic anhydride intermediate to desamido insulin and covalent dimer. Pharm Res 12: 1077–1084.
5. Strickley RG, Anderson BD. 1997. Solid-state stability of human insulin II. Effect of water on reactive intermediate partitioning in lyophiles from pH 2-5 solutions: Stabilization against covalent dimer formation. J Pharm Sci 86:645–653.
6. Darrington RT, Anderson BD. 1994. The The role of intramolecular nucleophilic catalysis and effects of self-association on the deamidation of human insulin at low pH. Pharm Res 11:784–793.

Q1: Please check the suitability of short title.
Q2: Please provide complete location.
Q3: Please provide complete location.
Q4: Please provide complete location.
Q5: Please update reference.

Comparison of the Glass Transition Temperature and Fragility Parameter of Isomalto-Olygomer Predicted by Molecular Dynamics Simulations with Those Measured by Differential Scanning Calorimetry

Sumie YOSHIOKA* and Yukio Aso

National Institute of Health Sciences; 1–18–1 Kamiyoga, Setagaya-ku, Tokyo 158–8501, Japan.
Received July 19, 2005; accepted August 21, 2005; published online August 23, 2005

The purpose of this study is to examine whether molecular dynamics (MD) simulations using a commercially available software for personal computers can estimate the glass transition temperature (T_g) of amorphous systems containing pharmaceutically-relevant excipients. MD simulations were carried out with an amorphous matrix model constructed from isomaltoheptaose, and the T_g estimated from the calculated density *versus* temperature profile was compared with the T_g measured by differential scanning calorimetry (DSC) for freeze-dried isomalto-oligomer having an average molecular weight close to that of isomaltoheptaose. The T_g values determined by DSC were lower by 10 to 20 K than those extrapolated from the T_g values estimated by MD simulation. Fragility parameter was estimated to be 56 and 51 from MD simulation and from DSC measurement, respectively. Thus, the results suggest that MD simulation can provide approximate estimates for the T_g and fragility parameter of amorphous formulations. However, a reduction of the cooling rate, achievable by sufficiently elongating the simulation duration, is necessary for more accurate estimation.

Key words molecular dynamics simulation; amorphous; glass transition; fragility; lyophilization

Glass transition temperature (T_g) is an important property for amorphous pharmaceutical formulations, because it is closely related to the storage stability. The T_g of amorphous materials can usually be determined by calorimetry, but this technique cannot be applied to amorphous formulations containing polymers with widely distributed molecular weights. This is because these formulations often exhibit unclear changes in heat capacity at T_g due to the glass transition occurring over a wide temperature range. Molecular dynamics (MD) simulations can be performed for an amorphous matrix model constructed using polymer molecules of a uniform molecular weight, in which the chemical structure of the repeated unit can be modified. If T_g prediction is possible based on MD simulations, the dependence of T_g on the polymer molecular weight as well as on the chemical structure of the repeated unit can therefore be elucidated, leading to the efficient development of polymer excipients with high T_g values suitable for stable amorphous dosage forms. Furthermore, MD simulations can determine the dependence of fragility for polymer matrices on the polymer molecular weight and on the chemical structure of the repeated unit. Thus, it would be possible to estimate the fragility parameter of polymer matrices with widely distributed molecular weights, which usually cannot be determined from the heating-rate dependence of T_g nor from the width of glass transition.

MD simulations have been utilized to estimate the glass transition temperature (T_g) of amorphous synthetic polymers,[1,2] glass former saccharides and concentrated saccharide–water systems.[3—8] These studies suggest that MD simulations are useful in estimating the T_g of amorphous materials. Our previous MD simulations with isomaltodecaose (a fragment of dextran) and α-glucose (the repeated unit of dextran) demonstrated that MD simulations can provide rational T_g values that decrease upon hydration and increase with increasing fragment size, suggesting the usefulness of MD simulations.[9] However, the T_g obtained from MD simulations was not compared with experimentally determined T_g, in consideration of the heating/cooling-rate dependence. Such comparison is necessary in order to evaluate the reliability of MD simulations.

In this study, the T_g of an isomalto-oligomer of relatively narrow molecular weight distribution was determined as a function of heating and cooling rates by differential scanning calorimetry (DSC). For the other angle of investigation, MD simulations were carried out with an amorphous matrix constructed from isomaltoheptaose, the molecular weight of which was close to the isomalto-oligomer investigated. The density of the isomaltoheptaose matrix was calculated as a function of temperature, and the T_g of the matrix was estimated from a change in the slope of the density *versus* temperature profile. The T_g estimates obtained at various cooling rates were compared with the experimental data in order to examine whether MD simulations using a commercially available software for personal computers can provide reliable T_g estimates for amorphous systems containing pharmaceutically-relevant excipients.

Experimental

DSC Measurement Isomalto-oligomer (number average molecular weight (Mn) of 1010; a polydispersity index (Mw/Mn) of 1.26) was purchased from Fluka Production GmbH (Switzerland). Four hundred microliters of 2.5% w/w isomalto-oligomer solution was frozen in a polypropylene sample tube (10 mm diameter) by immersion in liquid nitrogen for 10 min. Freeze drying was carried out at a vacuum level below 5 Pa for 23.5 h in a lyophilizer (Freezevac C-1, Tozai Tsusho Co., Tokyo). The shelf temperature was between −35 and −30 °C for the first 1 h, 20 °C for the subsequent 19 h, and 30 °C for the last 3.5 h. Residual water was less than the detection limit of the Karl Fisher method.

The T_g of lyophilized samples was measured by DSC (2920, TA Instruments, New Castle, DE, U.S.A.). Samples were heated in aluminum pans to 40 °C higher than the T_g, and then cooled to 40 °C lower than the T_g at a cooling rate of 2, 5 and 10 °C/min with a refrigeration system or at a cooling rate of 20 and 40 °C/min with a liquid nitrogen cooling accessory. Then, samples were heated again at a heating rate of 2, 5, 10, 20 and 40 °C/min. Temperature calibration was carried out using indium at each heating rate. The T_g was recorded as the middle of the change in heat capacity at the glass

* To whom correspondence should be addressed. e-mail: yoshioka@nihs.go.jp

transition.

Molecular Dynamics Simulation A model system for the amorphous isomalto-oligomer was built using the software package Amorphous Cell Construction (Material Studio, MSI Inc.). A periodic cell containing 7 isomaltoheptaose molecules was constructed by the minimization procedure using the Steepest Descents and Conjugate Gradients (5000 steps). For comparison with the isomaltoheptaose system, a periodic cell containing 49 α-glucose molecules was also constructed.

Isothermal-isobaric molecular dynamics simulations (NPTMD) were carried out with the constructed systems using the software package DISCOVER with the Polymer Consortium Force Field. The Velocity Verlet algorithm was used for integration. Interaction between non-bonded atoms was represented in van der Waals and Coulombic terms. Summation methods for van der Waals and Coulomb interactions were atom based and group based, respectively (cutoff of 12.50 A, spline width of 3.00 A, and buffer width of 1.00 A). Charge groups were defined in two different types. In type 1, the entire glucose unit was defined as a group. In type 2, five groups were defined (three groups were comprised of hydroxymethine at positions 2, 3 and 4, respectively, one group was comprised of C1, H1 and the ring O, and one group was comprised of the C5 methine, C6 methylene and O6), as shown in Chart 1. The different group definitions did not cause significant differences in the T_g values estimated, as described later.

A series of simulations was performed with temperatures decreased by intervals of 10 K from 673 to 353 K at a pressure of 0.1 MPa. Temperature and pressure were controlled by the Anderson procedure. The length of simulation at each temperature was 25, 100, 250 ps, or 1 ns with a step size of 1 fs, such that cooling rate was 0.4, 0.1, 0.04 or 0.01 K/ps, respectively. Each subsequent simulation was started from the final configuration obtained at the preceding temperature. System configurations were stored every 5000 steps. The density at each temperature was calculated from the average specific volume observed for the final third of the simulation span at the temperature. The series of simulations from 673 to 353 K was repeated 3 times

The calculated density was plotted against temperature, and the low-temperature and high-temperature portions of the data were fitted with straight lines. T_g was estimated from the point that deviated from the straight line in the low-temperature range and overlapped the straight line in the high-temperature range.

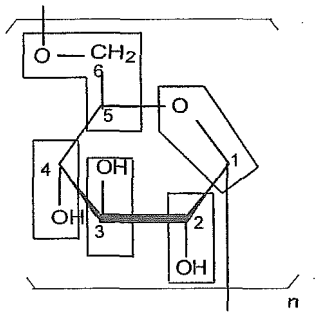

Chart 1. Five Charge Groups in the Repeated Unit of Isomaltoheptaose Defined for the Calculation of Coulomb Interaction

Results and Discussion

Figure 1 shows the density of the amorphous isomaltoheptaose system calculated by NPTMD at cooling rates of 0.4, 0.1, 0.04 and 0.01 K/ps as a function of temperature. The density *versus* temperature plots exhibit a change in the slope at a temperature corresponding to the T_g. As cooling rate decreased, variation in the density data decreased, showing more obvious changes in the slope.

T_g was estimated from the density *versus* temperature plots, and the results are plotted against cooling rate in Fig. 2. Figure 2 also shows T_g values measured by DSC for an isomalto-oligomer having a Mn of 1010 (close to the Mn of isomaltoheptaose, 1152). The T_g values measured during cooling were slightly lower than those measured during heating (the former overlapped with the latter at the two points of higher cooling/heating rate). The solid line in Fig. 2 represents a regression curve for the cooling-rate dependence of the T_g estimated by MD simulation (Type 1). The dotted line represents that of the T_g determined by DSC. Fragility parameters (m) were calculated according to Eq. 1[12] using the

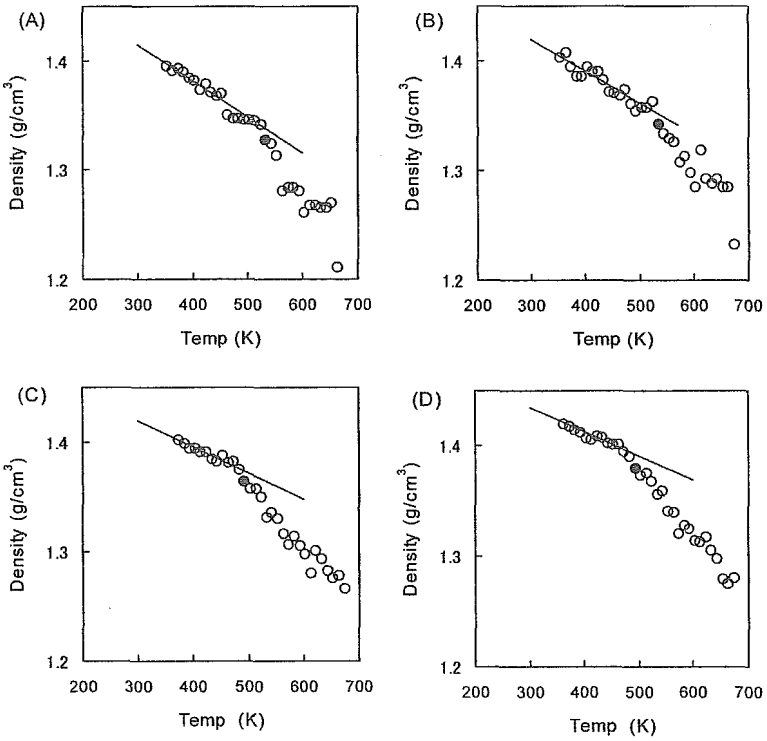

Fig. 1. Density *versus* Temperature Plots Obtained by NPTMD at Cooling Rates of 0.4 K/ps (A), 0.1 K/ps (B), 0.04 K/ps (C) and 0.01 K/ps (D)
Solid circles indicate estimated T_g.

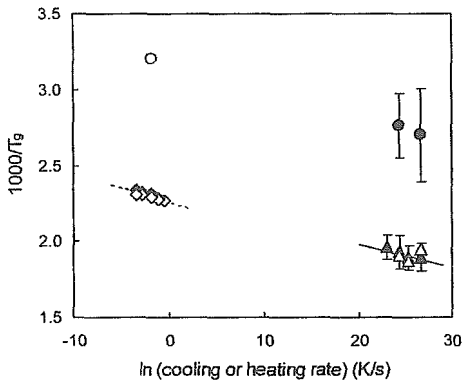

Fig. 2. Cooling-Rate Dependence of T_g Estimated from Density *versus* Temperature Plots for Amorphous α-Glucose (●) and Isomaltoheptaose (Type 1 Group ▲, Type 2 Group △) is Compared with the Heating-Rate Dependence of T_g Measured by DSC for Amorphous α-Glucose (○) and Isomalto-Oligomer (◇), and with the Cooling-Rate Dependence of T_g Measured by DSC for Amorphous Isomalto-Oligomer (◆)

The solid line and dotted line represent regression curves for the cooling-rate dependence of estimated T_g values and that of measured T_g values, respectively. Error bars for ● and ▲ represent S.D. (n=3).

slope of the regression curves and the T_g values at a cooling rate of 20 K/s (DSC measurement) and 4×10^{10} K/s (MD simulation).

$$m \cong \frac{1}{2.303T_g}\frac{d(\ln q)}{d(1/T_g)} \quad (1)$$

where q is the experimental heating or cooling rate. m was estimated to be 56 and 51 from MD simulation and from DSC determination, respectively. These values appeared to be reasonable in comparison with the values reported for various amorphous organic compounds.[12]

The dependence of T_g on the cooling rate (q) can be described by Eq. 2, if the relaxation time of the system shows a Vogel–Fulcher dependence on temperature.[13,14]

$$T_g = T_0 - \frac{B}{\ln(Aq)} \quad (2)$$

where A and B are constants and T_0 is the glass transition temperature when q approaches zero. Curve-fitting of the T_g estimated in the present MD simulation to Eq. 2 provided a regression curve shown in Fig. 3 (T_0, A and B were estimated to 421 K, 10^{-16} and 1150, respectively). The experimentally determined T_g values were lower than the extrapolated values by 10 to 20 K. This small difference suggests that MD simulation can provide approximate estimates of T_g and m, along with the fact that similar m values (56, 51) were estimated from MD simulation and from DSC measurement, respectively.

The lack of complete accordance between the T_g and m values estimated from MD simulation and those obtained from DSC measurement may be attributed to the short simulation duration (*i.e.*, the large cooling rate of 0.01—0.4 K/ps) used in the present study, in which density was not calculated at cooling rates slower than 0.01 K/ps because approximately 100 h of computing time were needed for an NPTMD of 1 ns duration. Decreasing the cooling rate (*i.e.*, prolonging the simulation duration) by using a more powerful computer would provide more reliable estimates of T_g and m. Furthermore, the difference between the estimated T_g and the experimentally determined T_g may result from the difference in parameter used in these two methods (*i.e.*, density in MD simulation *versus* heat capacity in DSC). Therefore, this effect needs to be elucidated for more precise estimation of T_g and m.

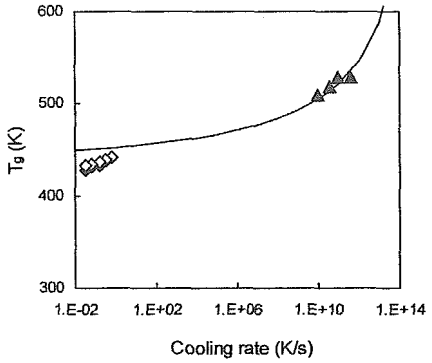

Fig. 3. Curve-Fitting of T_g Estimated from Density *versus* Temperature Plots for Isomaltoheptaose (Type 1 Group) ▲ According to Eq. 2

T_g for isomalto-oligomer determined by DSC during heating (◇) and during cooling (◆) are shown.

Figure 2 also compares the T_g of α-glucose measured by DSC with that estimated by MD simulation. The T_g estimates for α-glucose were lower than those for isomaltoheptaose, correctly reflecting a decrease in molecular weight. Although regression analysis could not be performed with this limited number of data, the relationship between the T_g from DSC measurement and from MD simulations appeared similar to that observed for the isomalto-oligomer.

Conclusions

The T_g of isomaltoheptaose estimated by MD simulation was compared with the T_g determined by DSC for isomalto-oligomer having a close Mn, in order to examine whether MD simulations using a commercially available software for personal computers can provide reliable T_g estimates of amorphous systems containing pharmaceutically-relevant excipients. The results suggest that MD simulation can provide approximate estimates for the T_g and m of amorphous formulations. However, a reduction of the cooling rate, achievable by sufficiently elongating the simulation duration, is necessary for more accurate estimation.

References

1) Han J., Gee R. H., Boyd R. H., *Macromolecules*, **27**, 7781—7784 (1994).
2) Tsige M., Taylor P. L., *Phys. Rev. E*, **65**, 021805-1-8 (2002).
3) Momany F. A., Willett J. L., *Biopolymers*, **63**, 99—110 (2002).
4) Conrad P. B., de Pablo J. J., *J. Phys. Chem. A*, **103**, 4049—4055 (1999).
5) Ekdawi-Sever N. C., Conrad P. B., de Pablo J. J., *J. Phys. Chem. A*, **105**, 734—742 (2001).
6) Caffarena E. R., Grigera J. R., *Carbohydr. Res.*, **315**, 63—69 (1999).
7) Caffarena E. R., Grigera J. R., *Carbohydr. Res.*, **300**, 51—57 (1997).
8) Roberts C. J., Debenedetti P. G., *J. Phys. Chem. B*, **103**, 7308—7318 (1999).
9) Yoshioka S., Aso Y., Kojima S., *Pharm. Res.*, **20**, 873—878 (2003).
10) Debenedett P. G., "Metastable Liquids, Consepts and Principles," Princeton University Press, Princeton, 1996.
11) Angell C. A., Torell L. M., *J. Chem. Phys.*, **78**, 937—945 (1983).
12) Crowley K. J., Zografi G., *Thermochimica Acta*, **380**, 79—93 (2001).
13) Vollmayr K., Kob W., Binder K., *J. Chem. Phys.*, **105**, 4714—4728 (1996).
14) Caprion D., Schober H. R., *J. Chem. Phys.*, **117**, 2814—2818 (2002).

Pharmaceutical Research, Vol. 22, No. 8, August 2005 (© 2005)
DOI: 10.1007/s11095-005-5262-z

Research Paper

A Quantitative Assessment of the Significance of Molecular Mobility as a Determinant for the Stability of Lyophilized Insulin Formulations

Sumie Yoshioka[1,2] and Yukio Aso[1]

Received October 24, 2004; accepted March 15, 2005

Purpose. The purpose was to explore a method for quantitatively assessing the contribution of molecular mobility to the chemical reactivity of amorphous solids. Degradation of insulin in lyophilized formulations containing trehalose and poly(vinylpyrrolidone)(PVP) was chosen as a model system, and the temperature- and glass transition temperature (T_g)-dependence of the degradation rate was analyzed to obtain the relative contributions of molecular mobility and that of the chemical activational barrier reflected in the energy of activation.

Methods. Insulin degradation and dimerization in lyophilized trehalose and PVP formulations were monitored at various relative humidities (6–60% RH) and temperatures (10–60°C) by reverse-phase high-performance liquid chromatography (HPLC) and high-performance size-exclusion chromatography (HP-SEC), respectively. The T_g and fragility parameter of the lyophilized insulin formulations were determined by differential scanning calorimetry (DSC).

Results. Insulin degradation in the initial stage was describable with first-order kinetics for both of the trehalose and PVP formulations. The temperature- and T_g-dependence of the degradation rate indicated that the reactivity of insulin in the trehalose formulation is affected by molecular mobility at low humidity (12% RH), such that the ratio of the observed rate constant (k′) to the rate constant governed only by the activational barrier (k) was 0.051 at the T_g. At higher humidities, in contrast, the value of k′/k was much higher (0.914, 0.978, and 0.994 for 23% RH, 33% RH, and 43% RH, respectively), indicating that insulin degradation rate is determined predominantly by the activational barrier. For insulin degradation in the PVP formulation at temperatures below T_g, the contribution of molecular mobility to the degradation rate appeared to be negligible, as the extrapolated value of t_{90} at the T_g exhibited a large difference between the formulations with differing T_g values (because of differing water contents).

Conclusions. The reactivity of insulin in the trehalose and PVP formulations can be described by an equation including factors reflecting the activational barrier (activation energy and frequency coefficient) and factors reflecting the molecular mobility (T_g, fragility parameter and a constant representing the relationship between the molecular mobility and the reaction rate). Thus, analysis of temperature dependence based on the proposed equation allows quantitative assessment of the significance of molecular mobility as a factor affecting chemical reactivity.

KEY WORDS: Adam-Gibbs-Vogel equation; glass transition temperature, insulin, lyophilized formulation; molecular mobility.

INTRODUCTION

Recent studies have demonstrated that molecular mobility is an important factor that affects the chemical (1–7) and physical (8–12) stability of amorphous pharmaceuticals including drugs of small molecular weight, peptides, and proteins (13–20). The contribution of molecular mobility to the rates of chemical degradations or physical changes such as crystallization is difficult to evaluate quantitatively, however, because thermodynamic factors also affect these rates. The chemical reactivity of amorphous solids is affected by molecular mobility as well as the chemical activational barrier, reflected in the energy of activation for the reaction. The contribution of molecular mobility to the reactivity has not been quantitatively evaluated in comparison with that of the activational barrier, however.

In formulation development and stability evaluation for amorphous pharmaceuticals, it is very important to assess the contribution of molecular mobility to the chemical reactivity. If the molecular mobility is found to be the predominant determinant of the reactivity, the chemical stability may be improved by increasing the glass transition temperature (T_g) using excipients with high T_g. If the contribution of molecular mobility to the reactivity is negligible, stability prediction by extrapolating stability data obtained under accelerated con-

[1] National Institute of Health Sciences, Setagaya-ku, Tokyo 158-8501, Japan.
[2] To whom correspondence should be addressed. (e-mail: yoshioka@nihs.go.jp)

ABBREVIATIONS: DSC, differential scanning calorimetry; HPLC, high-performance liquid chromatography; HP-SEC, high-performance size-exclusion chromatography; PVP, poly(vinylpyrrolidone); RH, relative humidity; RP-HPLC, reverse-phase HPLC.

ditions may be possible even if the extrapolation extends across the T_g.

In this study, we explored a method for quantitatively assessing the significance of molecular mobility as a factor affecting chemical reactivity. Degradation of insulin in lyophilized formulations containing either trehalose or poly (vinylpyrrolidone)(PVP) was chosen as a model system, and the temperature- and T_g-dependence of the degradation rate was analyzed to obtain the relative contributions of molecular mobility and that of the activational barrier. It is well known that the major degradation pathways of insulin in solution and in the solid state are deamidation and dimerization via a cyclic imide intermediate (14,21–23).

MATERIALS AND METHODS

Preparation of Lyophilized Insulin Formulation

Human zinc insulin (Humulin® RU-100) was purchased from Eli Lilly & Co, and converted into the zinc-free neutral form by dialysis as reported (24). Trehalose (203-02252) or PVP (K-30, Wako Pure Chemical Ind. Ltd., Osaka) was dissolved in the zinc-free insulin solution to make a 5 mg/ml solution, and the pH was adjusted to 4.0. The resulting solution contained insulin and trehalose or PVP (1:1.5 w/w). Four hundred microliters of the solution were frozen in a polypropylene sample tube (10 mm diameter), and then dried at a vacuum level below 5 Pa for 23.5 h in a lyophilizer (Freezevac C-1, Tozai Tsusho Co., Tokyo). The shelf temperature was between −35 and −30°C for the first 1 h, 20°C for the subsequent 19 h, and 30°C for the last 3.5 h.

Lyophilized samples with various water contents were obtained by storage at 15°C for 24 h in a desiccator with a saturated solution of $LiBr \cdot H_2O$ [6% relative humidity (RH)], $LiCl \cdot H_2O$ (12% RH), potassium acetate (23% RH), $MgCl_2 \cdot 6H_2O$ (33% RH), $K_2CO_3 \cdot 2H_2O$ (43% RH) or $NaBr \cdot 2H_2O$ (60% RH).

Determination of T_g and Fragility Parameter by Differential Scanning Calorimetry (DSC)

Lyophilized samples with various water contents were placed in a hermetic pan, and thermograms were obtained in the temperature range from 40°C lower than the T_g to 40°C higher than the T_g at a heating scan rate of 5°C/min (2920; TA Instruments, DE). Temperature calibration was performed using indium. The measured T_g values are shown in Table I. The fragility parameter (m) for the trehalose formulation was calculated from the glass transition width determined from the extrapolated onset and offset (25,26). The calculated m value was 45 and 50 at 12% RH and 43% RH, respectively.

Table I. The T_g of lyophilized insulin formulations determined by DSC

	T_g (°C)	
Relative humidity (% RH)	Trehalose	PVP
6	—	160
12	44	129
23	26	103
33	10	85
43	0.8	80
60	—	56

—, Not determined.

Determination of Insulin Degradation and Dimerization Rates

Lyophilized samples containing various amounts of water were stored in tightly screw-capped tubes at a constant temperature (10–60°C), removed at various times, and stored in liquid nitrogen until assayed. Samples were dissolved in 1.5 ml of 0.01 M $(NH_4)_2SO_4$ (pH 2.2, adjusted with concentrated H_2SO_4) and subjected to reverse-phase high-performance liquid chromatography (RP-HPLC) and high-performance size-exclusion chromatography (HP-SEC).

The concentration of intact insulin was quantified using a modular RP-HPLC consisting of two Shimadzu pumps with a mixer (LC-10AD), an injector (SIL-10ADVP), and a UV detector (SPD-10A), as reported (27). The column used was Inertsil WP-300 (C8, 4.6 mm × 250 mm, GL Science Inc.) maintained at 35°C. Elutions were performed using a mixture of 0.01 M $(NH_4)_2SO_4$ (pH 2.2, adjusted with concentrated H_2SO_4) and acetonitrile solution of 0.07% (v/v) trifluoroacetic acid (72.5:27.5) for 1 min. The ratio of the acetonitrile solution increased linearly from 27.5% to 30% in 15 min and 30% to 35% in 22 min. The detection wavelength was 214 nm.

Higher molecular weight transformation was determined by HP-SEC, using a Hitachi UV detector (L-4000) and a column (Protein-Pak 125, 7.8 mm × 300 mm, Waters) maintained at 25°C, as reported (21). A 2.5 M acetic acid solution containing 4 mM L-arginine and 4% (v/v) acetonitrile was eluted at a rate of 1 ml/min. The amount of insulin within an intact molecule of a given size was measured based on the peak height.

RESULTS AND DISCUSSION

Figure 1 shows the time courses of insulin degradation at 43% RH in the PVP formulation determined by RP-HPLC. Similar time courses were also obtained at 6% RH, 12% RH, 23% RH, 33% RH, and 60% RH in the PVP formulation, and at 12% RH, 23% RH, 33% RH, and 43% RH in the trehalose formulation. The major degradation pathway is known to be deamidation through a cyclic imide intermediate (14,21–23). Degradation in the initial stage was describable with first-order kinetics for both of the trehalose and PVP formulations. The time required for 10% degradation (t_{90}) was calculated from the apparent first-order rate constant. Time courses of insulin dimerization determined by HP-SEC were also describable with first-order kinetics in the initial stage (data are not shown).

Figure 2 shows the temperature dependence of the calculated t_{90} for insulin degradation and dimerization. For

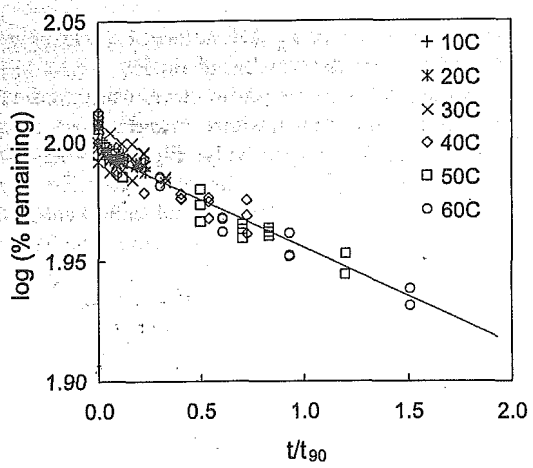

Fig. 1. Time courses of insulin degradation in PVP formulation at 43% RH at various temperatures. Time is scaled to the t_{90} for each temperature.

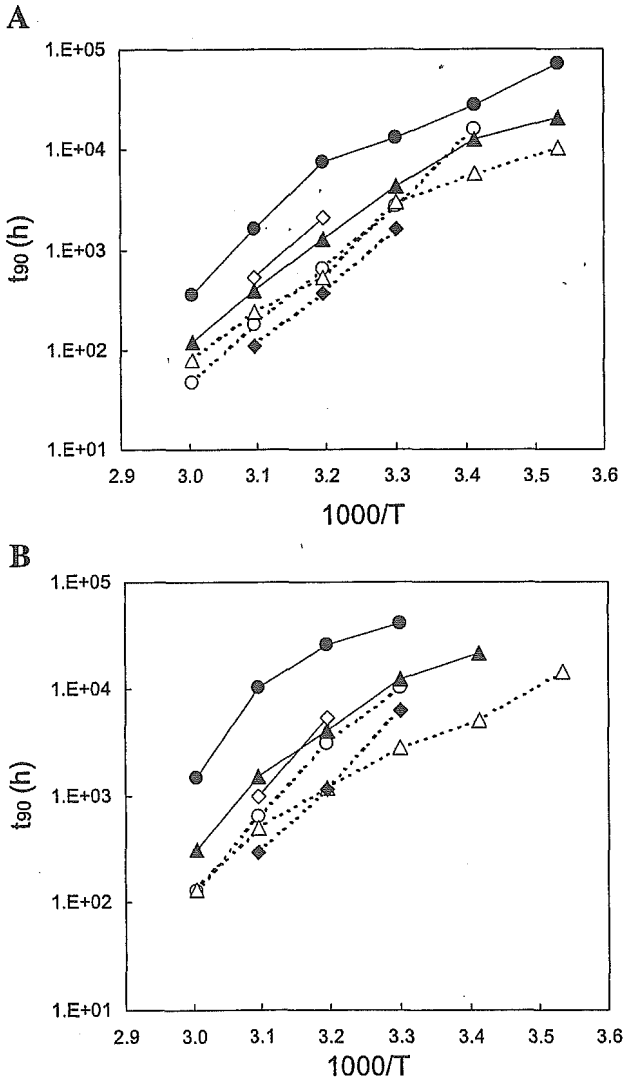

Fig. 2. Temperature dependence of t_{90} for insulin degradation (A) and dimerization (B). (●) trehalose at 12% RH; (◇) trehalose 23% RH; (○) trehalose at 33% RH; (◆) trehalose 43% RH; (▲) PVP at 12% RH; (△) PVP at 43% RH.

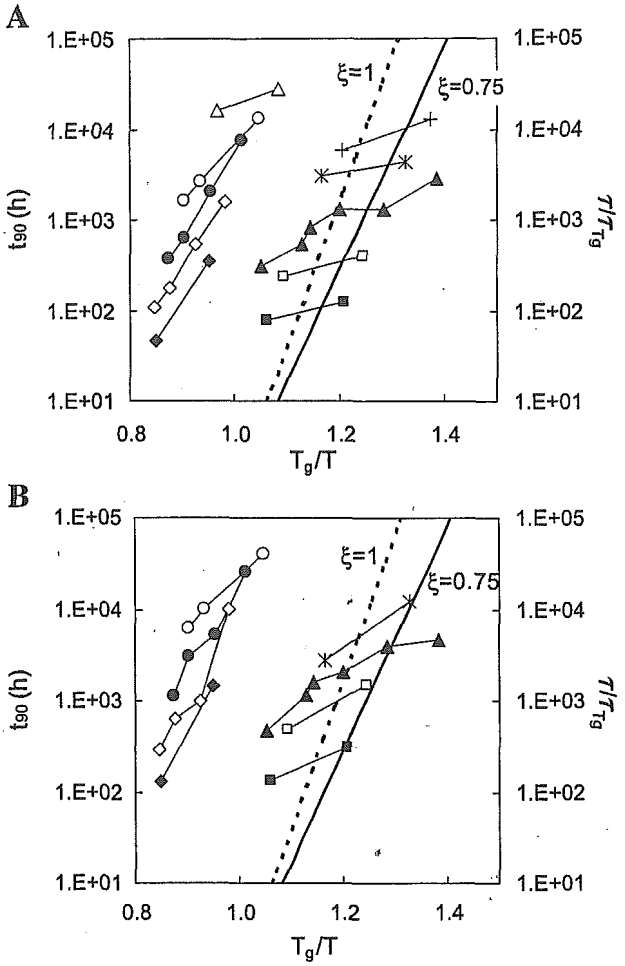

Fig. 3. T_g dependence of t_{90} determined at a constant temperature for insulin degradation (A) and dimerization (B). Trehalose at various RHs (12% RH–43% RH) at 60°C (◆), 50°C (◇), 40°C (●); 30°C (○), and 20°C (△); PVP at various RHs (6% RH–60% RH) at 60°C (■), 50°C (□), 40°C (▲), 30°C (✳), and 20°C (+). Dotted and solid bold lines represent the structural relaxation time calculated according to the AGV equation using ξ = 1 and 0.75, respectively.

both of the trehalose and PVP formulations, t_{90} was larger at lower humidity. Comparison of t_{90} at 12% RH indicated that the trehalose formulation was more stable than the PVP formulation. This difference in t_{90} between the trehalose and PVP formulations decreased at 43% RH.

Figure 3 shows the T_g dependence of t_{90} obtained at a constant temperature (20–60°C). For both of the trehalose and PVP formulations, t_{90} increased with increasing T_g associated with decreasing water content. The trehalose formulation exhibited a t_{90} at T_g that was approximately two orders of magnitude larger than the PVP formulation for insulin degradation and dimerization at 40°C.

Simulations of the Effect of T_g, ΔH, and α on t_{90}

For a reaction occurring in the physical state in which the rate-determining step involves molecular diffusion (e.g., in the solid state), the rate constant (k′) can be related to the rate constant at the condition under which reactants have